

RESEARCH ARTICLE

Crystals for neutron scattering studies of quantum magnetism

T. Yankova*, D. Hübner, S. Mühlbauer, D. Schmidiger,
E. Wulf, S. Zhao and A. Zheludev†

*Neutron Scattering and Magnetism Group, Institute for Solid State Physics, ETH Zürich,
Switzerland.*

T. Hong, V. O. Garlea, R. Custelcean and G. Ehlers
Oak Ridge National Laboratory, Oak Ridge, TN, USA.

(October 31, 2018)

We review a strategy for targeted synthesis of large single crystal samples of prototype quantum magnets for inelastic neutron scattering experiments. Four case studies of organic copper halogenide $S = 1/2$ systems are presented. They are meant to illustrate that exciting experimental results pertaining to forefront many-body quantum physics can be obtained on samples grown using very simple techniques, standard laboratory equipment, and almost no experience in advanced crystal growth techniques.

Keywords: transition metal halogenides; quantum magnetism; neutron scattering; single crystals; spin chains, spin ladders

1. Introduction

For the past 50 years, neutron spectroscopy has been one of the most powerful tools for the study of local and collective excitations in condensed matter systems [1]. Virtually all that we know of phonons and magnons comes from such experiments. Most other techniques are not momentum resolved and provide only very limited and indirect information. Other methods are restricted to looking at the charge sector, and are not suited for the study of magnetism and nucleus dynamics. Still others can only probe surface properties.

Arguably, the main limitation of neutron spectroscopy is the need for very large single crystal samples, typically of a few grams or even tens of grams. Until roughly the mid-90s, this created a very interesting synergy between crystal growers and expert neutron scatterers. The complexity of neutron instrumentation and data analysis, and the fact that neutrons are only produced at dedicated large-scale installations, ensured that these were two distinct groups of scientists. They were even separated geographically: the former were typically at universities, while the latter concentrated at the facilities.

In the past fifteen years the situation has changed drastically. Many neutron techniques are now mature, well tested and fully optimized. Instruments and data analysis software have evolved to be accessible to the non-expert. Most importantly, most neutron scattering facilities such as Institut Laue Langevin, ISIS and

*Permanent address: Chemistry Department, Moscow State University, Moscow, Russia.

† Corresponding author. Email: zhelud@ethz.ch.

the Spallation Neutron Source now run extensive programs to support external users. Crystal growers nowadays can run their own neutron experiments, while the neutron scattering experts serve them as hosts and local contacts. Of course, not all experiments can be carried out in this mode by non-experts, but *many* can.

What is a “professional” neutron scatterer to do, to maintain a competitive research program of his or her own? A winning strategy is to grow his or her own samples. Of course, not all materials can be grown into large single crystals by a non-expert, but *many* can. This paper is a case study. We show how a team of hardcore neutron scatterers working in the rather esoteric field of quantum magnetism can greatly benefit from investing just a little of their time in crystal growth.

1.1. Challenges in quantum magnetism

“Quantum magnets” are defined as magnetic materials in which long-range magnetic order is destroyed even at zero temperature by anomalously strong quantum spin fluctuations. Many low-dimensional and geometrically frustrated antiferromagnets (AFs) fall into this category. Since there is no long range magnetic order, *all* the information on the physics of these materials is contained in excitations. Examples include the AF Heisenberg spin chains [2] (including so-called Haldane chains [3]), spin ladders [4], bond-alternating chains [5], and more complex frustrated geometries [6].

Neutron spectroscopy, being able to probe spin excitations at non-zero momenta, played a particularly important role in understanding the exotic and complicated many body quantum mechanics on these materials. Initially, most studies were performed on transition metal oxide systems. Among the examples are the Haldane spin chain compound Y_2BaNiO_5 , the spin chain system SrCuO_2 [7] and the exotic spin ladder $\text{La}_4\text{Sr}_{10}\text{Cu}_{24}\text{O}_{41}$ [8]. Unfortunately, the rather large energy scale of magnetic interactions in such materials (typically 10–1000 meV) prohibits the study of finite-temperature effects ($\kappa_B T \lesssim 30$ meV) and the extremely interesting new physics [9] that emerges in applied external magnetic fields ($g\mu_B H \lesssim 2$ meV). Recent breakthroughs were therefore achieved in studies of organic quantum magnets, particularly in transition metal complexes. Among these compounds, for neutron experiments, one finds excellent one-dimensional [10–14] and two-dimensional [15–17] spin networks with varying degrees of geometric frustration [15, 18] and typical magnetic energy scales of 1 meV. These energies correspond to temperatures [19–22] and magnetic fields [23–27] that can be realized in neutron experiments. They are also perfectly suited for spectroscopic studies with low-energy neutrons ($\lambda \sim 5$ Å). Moreover, the use of cold neutrons often helps avoid background due to phonon scattering, and for a number of technical reasons allows a cleaner measurement of the spin excitations. In addition to temperature- and field-dependent studies of quantum magnets, there is a growing interest in the effects of disorder. For these applications too, transition metal organic complexes are excellent models: chemical disorder is easy to introduce on either the magnetic [28–30] or non-magnetic [31–34] sites.

From the practical point of view of the neutron scatterer who aspires to synthesize his or her own samples, transition metal organic complexes often have the advantage of being easy to grow. In this work we shall specifically focus on organic halogenides, for which very large and nicely faceted single crystals can be obtained in many cases. The growth is typically done in solution, and requires no special equipment beyond that found in a typical wet chemistry laboratory. Even physics students with minimal experience in material science or chemistry can have the privilege of growing (and modifying, and controlling) their own samples for neu-

tron experiments.

1.2. Methods

The peculiarities of neutron scattering impose specific requirements on the samples used. As mentioned, large single crystals are a necessity. Being large in volume, they should be rather compact. The typical neutron beam cross section is only about 2 cm, and the sample should be fully immersed. Long needles or thin platelets are not particularly useful. Fortunately, for spectroscopy experiments, the quality of the crystals is less critical than one may expect. A mosaic spread of 2° or even larger is acceptable. Several grains aligned within this tolerance can be treated as a “single” crystal. Diffraction is more demanding, but even there a symmetric mosaic spread of 0.5° can often be tolerated. The neutron scattering and absorption cross sections are strongly isotope-dependent [35]. Hydrogen, for example, is pernicious for neutron experiments due to its enormous incoherent cross section. Incoherent scattering contributes to background and removes neutrons from the incident beam. The neutron penetration depth in a proton-containing sample is typically only a few millimeters. Thus, in most cases, hydrogen-bearing samples for neutron experiments must be deuterated. As will be illustrated in one example below, partial deuteration is of not much use, and one typically tries to substitute at least 95% of all hydrogen sites with deuterium (more is better). There are a few other “taboo” isotopes besides hydrogen [36]. Among them are ^{10}B , natural Gd and natural Cd, due to their huge absorption cross sections for thermal neutrons.

By far, the easiest way to produce neutron-specific crystals is by solution growth. Since it occurs at conditions close to equilibrium, high-quality large crystals can be obtained. Low temperature solution growth is particularly useful and versatile [37]. It is cheap, simple and relatively safe. This technique also has the obvious advantage for crystals that are unstable at high temperatures. Such are the transition metal organic complexes that are a focus of this work. Several methods of low-temperature solution growth can be classified: (i) slow cooling, (ii) slow evaporation, (iii) the temperature gradient method, and (iv) the chemical/gel method [37]. Only the

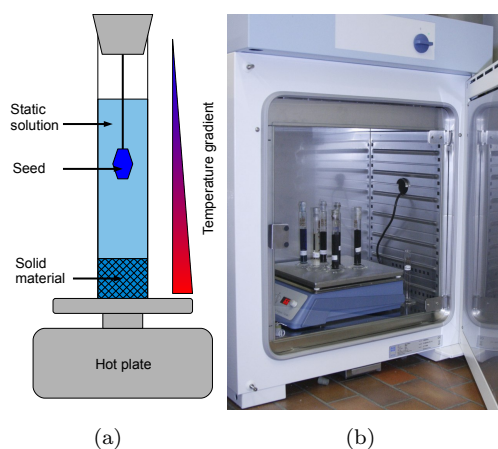


Figure 1. (Temperature gradient growth of single crystals: (a) Schematic of the setup. (b) Refrigerated environmental chamber with several crystallization cylinders on a hotplate.

slow evaporation and temperature gradient methods are discussed here.

1.2.1. Slow evaporation

Slow evaporation is useful for materials with a low temperature coefficient of solubility. The growth occurs at a fixed temperature. Due to the higher stability one can, in principle, expect larger and better crystals than those obtained with slow cooling. The slow evaporation method is very straightforward to realize. The key requirement is high temperature stability. In our laboratory at ETH Zurich it is achieved in commercial environmental chambers such as the Friocell models by Medcenter Einrichtung GmbH. The crystallization beakers are set up inside

airtight containers (we use standard glass dessicators), which are in turned placed in the environmental chambers.

The removal of solvent vapors is performed in a controlled way, by flowing nitrogen gas through the dessicators. The gas flow rate is controlled by automated metering valves. The nitrogen and solvent vapor exhaust is released into an acid hood. One of the many advantages of this setup is the use of dry nitrogen gas that prevents environmental water vapor from entering the growth solution. Besides disrupting the growth balance, such water brings in hydrogen ions. The latter can exchange with deuterium ions of the growing crystal, which, for neutron scattering purposes, is to be avoided. Some solvents are not particularly hygroscopic, and many crystals will grow without a highly stable environment. In these cases one can simply leave the growth beaker under an acid hood and allow evaporation to take its course in an uncontrolled manner.

To obtain large crystals, seeds are first precipitated by slow evaporation of a saturated solution. The best seeds are then suspended on PTFE threads in a solution that is filtered and saturated at the evaporation temperature. In our experiments the latter varies between 20°C to 60°C, depending on the substance to be grown and the solvent used. The crystal growth rate and quality are controlled by temperature, nitrogen flow and aperture of the growth beaker. Optimal growth parameters are determined by trial and error, and luck is always an important ingredient.

1.2.2. *Temperature gradient*

The main disadvantage of evaporative growth for our applications is the loss of solvent. Deuterated organic solvents can be extremely expensive and are to be conserved. Our attempts to recover solvent vapor from the nitrogen exhaust using a Peltier-cooled condenser were only partially successful. A totally different approach, namely the temperature gradient method, is in many cases a better alternative. In this technique, a thermal gradient is maintained across the growth solution. Assuming that solubility increases with temperature, an excess of the solute is placed in the hotter region. The growth compound is transported through the solution to a cooler region. Here the solution becomes over-saturated and crystals are precipitated. The transport is usually due to thermal convection, but can also be diffusive.

In our setup, we use volumetrical cylinders of volume 25 ml or 50 ml. As a first step, powder and seeds of the target compound are obtained by slow evaporation. Some solid target material is placed on the bottom of the growth cylinder and topped off with 25–50 ml of the saturated solution. The seed is suspended in the upper region of the cylinder, which is then sealed. A temperature gradient is achieved by heating of the cylinder bottom on a hotplate (Fig. ??a). For stability, the hotplate is placed into a refrigerated environmental chamber. Active refrigeration is necessary to drain the heat released by the hotplate and ensure a relatively low temperature for upper part of the cylinder. Typical chamber temperatures are 30°C, with hotplate temperatures varying between 50°C to 160°C, depending on the substances involved. Such a setup is illustrated in Fig. ??b. Besides totally eliminating the loss of solvent, this method provides isolation from any detrimental environmental factors.

1.2.3. *Introducing disorder*

Among the issues that we address in the present study is the effect of magnetic bond strength disorder on the properties and excitation spectra of quantum spin systems. In our experiments on organic copper halogenides, disorder is introduced by a partial chemical substitution on the halogen sites. Crystals of such materials are prepared by adding the corresponding reagents to the growth solution. For

example, instead of copper (II) chloride we use the same molar amount of a mixture of copper (II) chloride and bromide. The method works particularly well for partial substitution of Cl by Br and *vice versa*, thanks to the similarity of the corresponding ionic radii. The crystal growth procedures are the same as for disorder-free parent compounds.



Figure 2. Four deuterated crystals wrapped in PTFE film and wired down on an aluminium sample holder for a total mosaic spread of about 1° . The use of perforated aluminium reduces the amount of material in the beam. A small amount of glue visible near the base of the holder is permissible, as it remains outside the neutron beam. In this case, a stringent constraint on sample diameter is imposed by the use of a ^3He - ^4He dilution refrigerator to achieve $T < 100$ mK required for some experiments.

to be less precise for small concentrations. A common concern is whether halogen concentrations remain uniform even in very large crystals. To within the experimental error of our chemical analysis, this appears to be the case for all materials discussed here. In some cases, this conclusion can also be drawn from the sharpness of magnetic phase transitions observed with neutron diffraction.

1.2.4. Preparing the crystals for experiment

A few words need to be said about mounting the single crystals for neutron scattering experiments. First, they need to be aligned in a particular orientation to within a couple of degrees. Having nicely faceted crystals that are often the result of solution growth, helps with this task. The alignment can be done with X-ray Laue diffraction or using a single-crystal diffractometer. Even if X-rays are used, the final test is to be done with neutrons, since only neutrons can penetrate the bulk of the crystal and reveal hidden misaligned grains. Very often several separate crystals can be co-aligned to produce a larger volume “supersample”. The sample mounts for neutron experiments are typically made of aluminium or copper, which are largely transparent for neutrons and have good thermal conductivity. Even so,

Typically, substitution at concentrations of up to 10 at.% is relatively easy to achieve. Crystal growth at higher concentration is often inhibited. We speculate that this is due to large lattice strains that emerge when at high concentrations two or more ions of the “wrong” radius are forced on adjacent sites. In general, the higher the substitution level, the lower the growth rate and the lower the quality of the resulting crystals. In some cases, the introduction of foreign halogen ions leads to the formation of entirely different and typically useless (from the physics point of view) crystallographic phases. It can also happen that only one stoichiometric material will grow even from a mixture containing different halogen species.

The nominal concentration of halogen-site substitute in solution can be different from that in the resulting crystal. Fortunately, our organic systems involve mostly light elements. As a result, the contrast between Cl and Br is sufficient to determine the concentrations with X-ray diffraction. Such studies are performed using a small-molecule single crystal diffractometer. In our ETH Zurich laboratory we employ the Bruker APEX II system. Often, the Br or Cl content can be determined to within a fraction of a percent. For a cross-check we also use micro-elemental analysis (Schoeniger method), but that tends

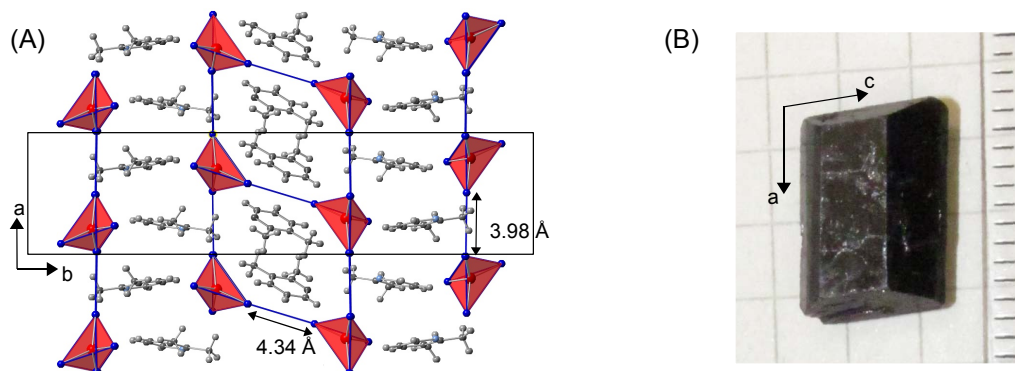


Figure 3. (A) Crystallographic structure of DIMPY seen along the c -axis: The Cu^{2+} -ions are colored in red, the Br^- ions in blue. The CuBr_4^{2-} tetrahedra are shaded in red. The organic spacer molecule is shown in gray. The blue lines indicate the spin ladder structure. (B) Fully deuterated single crystal of DIMPY with a size of $\approx 11 \times 8 \times 5 \text{ mm}^3$.

scattering from either metal can contribute to the background, and Cu is slightly absorbing. Therefore, as little material as possible is to be used. To avoid introducing hydrogen in the beam, no conventional glue can ever be applied! Instead, the crystals are attached with thin aluminium wire or PTFE film (plumbing tape). PTFE is hydrogen-free and produces surprisingly little incoherent neutron background.

Assembling and aligning such samples may take hours or even days of work in the neutron beam (triclinic crystals are the hardest to deal with). This implies exposing the crystals to the atmosphere. Sample stability and hygroscopicity become serious issues. Some of our organic copper (II) halogenides are unstable, being hygroscopic or losing solvent that is part of their crystal structure to evaporation. In addition, all of them are corrosive materials and may react with the sample holders. Several strategies can be used to protect the crystals. Tightly wrapping them in PTFE helps, as does dipping crystals into PFPE lubricants such as Fomblin. An example of four co-aligned crystals ready for neutron experiments is shown in Fig. 2.

2. Case studies

2.1. A strong-leg spin ladder

The antiferromagnetic $S = 1/2$ Heisenberg two leg ladder is probably the most famous model in quantum magnetism. It exhibits a gapped, spin-liquid ground state with sharp triplet excitations. It can be intuitively understood in two different coupling limits. A *strong-rung* ladder is essentially a system of weakly coupled dimers. In contrast, the more interesting *strong-leg* ladder is described as weakly interacting quantum spin chains. Until the discovery of the *strong-rung* spin ladder material $(\text{C}_5\text{H}_{12}\text{N})_2\text{CuBr}_4$ (Hpip) [38], most known ladders were cuprates with large intrinsic energy scales [39]. The low energy scales of organometallic Hpip for the first time opened experimental access the entire magnetic phase diagram [27, 40, 41], but obviously only in the strong-rung limit.

The first realization of a *strong-leg organometallic* Heisenberg spin ladder is the compound Bis(2,3-dimethylpyridinium)-Tetrabromocuprate (DIMPY) [42, 43]. DIMPY crystallizes in the monoclinic space group $P2_1/n$ with lattice parameters $a = 7.504 \text{ \AA}$, $b = 31.61 \text{ \AA}$, $c = 8.202 \text{ \AA}$ and $\beta = 98.97^\circ$. The magnetic behavior is governed by the Cu^{2+} -ions in a ladder structure composed of CuBr_4^{2-} tetrahedra. The Cu^{2+} -ions are interacting via nearest neighbor Cu-Br \cdots Br-Cu AF su-

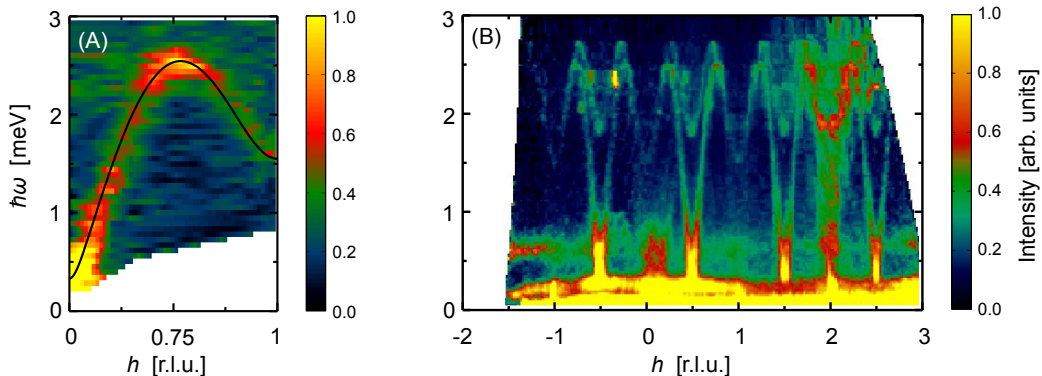


Figure 4. (A) False color map of the spin excitation spectrum in DIMPY composed of individual constant- q scans measured along the line $\mathbf{q} = (h, 0, 0.17 - 1.44 \cdot h)$ for $0.5 < h < 1$, $T = 50$ mK. The data are from [44]. (B) False color projection of the spectrum measured on in time-of-flight mode at $T = 2$ K [45].

perexchange. The unit cell and the spin ladder structure is shown in Fig. 3(A). Measurements of susceptibility [42] and specific heat [34] are consistent with a spin ladder in the *strong-leg* regime. The spin excitation spectrum was studied by inelastic neutron scattering on a partially (67%) deuterated single crystal sample and confirmed a spin gap of $\Delta = 0.32(2)$ meV [34]. However, due to the strong incoherent scattering from hydrogen, the magnons could be only observed at large wavelengths, close to the antiferromagnetic zone center. It became clear that no further progress can be made without *fully deuterated* single crystal samples.

Such high quality fully deuterated (98 at.% D) single crystals of DIMPY were successfully grown in our laboratory at ETHZ using the temperature gradient method. Due to the high costs, the growth recipe has been optimized to use as little deuterated reagents as possible: 0.03356 mole (3.75 g) of deuterated 2,3-Lutidine (C_7D_9N), 0.03356 mole of 4.5 M deuterobromic acid (DBr) and 0.01668 mole (3.727 g) of high purity water free $CuBr_2$ are consecutively dissolved in 30 ml of ethanol- d_6 while stirring at $50^\circ C$. A dark violet solution is obtained. After stirring for 24 hours in a sealed container, the solution is slowly evaporated and 10 g of dry DIMPY powder is harvested. 7 g of the powder is redissolved in a 25 ml cylinder with 22 ml ethanol- d_6 . The result is a saturated solution with ≈ 3 g of undissolved DIMPY at the bottom of the cylinder. The growth is performed with the temperature gradient method at a base temperature of $65^\circ C$ and ambient temperature of $30^\circ C$. The seeds were separately obtained by the slow diffusion method. After two months, single crystals with a mass of 1 g – 1.5 g are harvested. After refilling DIMPY powder to maintain a saturated solution the growth procedure can be repeated several times. The crystals show a dark violet to black color and clean facets. Fig. 3(B) depicts a typical single crystal with a mass of ≈ 1 g. The crystalline structure and quality were confirmed with single crystal X-ray and neutron diffraction, revealing a mosaic spread of 0.45° FWHM and no signs of parasitic phases.

Experiments on these highly deuterated samples, some still ongoing, are providing new insight on the physics of quantum spin ladders. We are utilizing four co-aligned crystals with a total mass of 3.7 g (Fig. 2). The initial data were collected on the triple axis spectrometer TASP at Paul Scherrer Institut, Villigen, Switzerland. The spectrum measured at $T = 50$ mK is shown in Fig. 4(A). It reveals that the single-magnon excitations remain sharp throughout the entire Brillouin zone. This confirms a peculiar symmetry of the ladder spin Hamiltonian which is invariant under leg permutation [44]. In a previously studied asymmetric ladder the magnons become unstable at certain wave vectors[13].

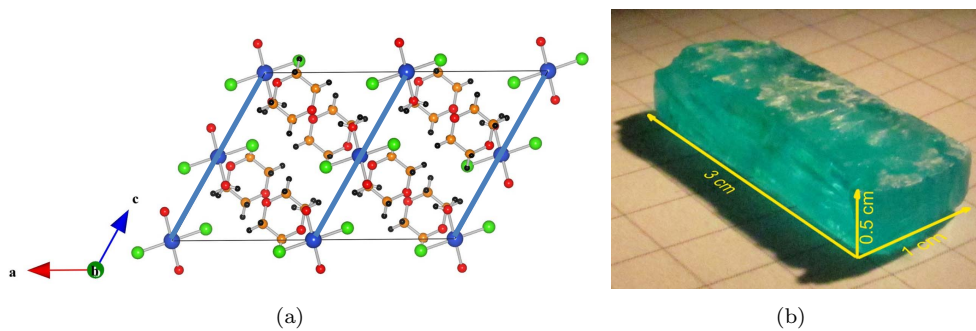


Figure 5. (a) View along the crystallographic b axis showing how Cu^{2+} ions are linked into a one-dimensional chain. The chain axis is along the crystallographic c direction. The chains are well separated by 1,4-Dioxane molecules. Color coding is as follows: Blue:Cu, Green:Cl, Orange:C, Black: H, and Red:O. (b) Shape of a typical 2Dioxane·2D₂O·CuCl₂ single crystal grown from aqueous solution with slow evaporation method.

The most recent experiments were carried out at the Cold Neutron Chopper Spectrometer CNCS [46] at Oak Ridge National Laboratory and revealed stunning new details [45]. A projection of the 4-dimensional data set onto the energy- leg momentum axes recorded during a single day on of measurement is shown in Fig. 4(B). Even without background subtraction and further analysis, one notices an addition sharp excitation branch. Theoretical and numerical studies allowed us to identify this mode with a novel two-magnon bound state [45]. A more thorough data reduction and new experiments in high magnetic fields are underway, fully justifying the effort and expense of preparing deuterated crystals.

2.2. An accidental discovery: an almost perfect $S = 1/2$ spin chain

Solution growth can sometimes produce unexpected results. It was reported by Ajiro *et al.* that the material 2Dioxane·3CuCl₂ realizes a peculiar ferro-ferro-antiferromagnetic (FFA) Heisenberg $S = 1/2$ chain [47]. With the aim to further investigate this famous model, at ORNL we set out to prepare samples following the procedure described in [48]. The resulting single crystals seemed to match the description and bulk properties reported in Ajiro's work. However, once we invested in high-purity deuterated reagents to grow crystals for neutron scattering, we suddenly were unable to reproduce the synthesis. The mystery was solved by studying the original non-deuterated samples with X-ray diffraction. The data collected on a Bruker SMART Apex diffractometer revealed that, in fact, a novel compound, 2Dioxane·2H₂O·CuCl₂ was obtained. It appears, that the necessary water entered the growth solution from the atmosphere or through the use of low-quality ethanol or methanol solvent. Once a small amount of heavy water was added to our deuterated reagents, obtaining large crystals was straightforward.

The slow evaporation growth procedure can be summarized as follows. 3.56 grams of anhydrous CuCl₂ is dissolved in 60 ml of deuterated anhydrous methanol inside a beaker with stirring. 100 ml of deuterated 1,4-Dioxane and 8 ml of D₂O are separately slowly added consecutively with stirring. The growth beaker is covered leaving a few pinhole openings. Nicely shaped blue crystals are harvested after a few weeks. Seeds obtained in this manner can be suspended on a PTFE filament in the growth solution and further enlarged. Ultimately, at the laboratory at ETHZ, deuterated crystals of up to several grams each were successfully grown (Fig. 5(b)).

Obviously, the new material does not have the unique FFA chain motif. The crystal structure of 2Dioxane·2H₂O·CuCl₂ is monoclinic, with space group $C2/c$ and lattice constants $a=17.4298(9)$ Å, $b=7.4770(4)$ Å, $c=11.8230(6)$ Å, and

$\beta=119.4210(10)^\circ$. It consists of $\text{CuCl}_2 \cdot 2\text{H}_2\text{O}$ bi-layers in the (a, c) plane. These layers are well separated from one another by the 1,4-Dioxane molecules. The copper ions form simple chains along the crystallographic c direction as shown in Fig. 5(a). Intra-chain magnetic coupling is antiferromagnetic and involves Cu-Cl-H-O-Cu super-exchange pathway.

Crystals of the new material turned out to be unstable in atmosphere, rapidly losing 1,4-Dioxane to evaporation. Even large crystals deteriorate in a matter of a few hours. We believe that a partial decomposition of the sample led to the original misinterpretation of bulk magnetic measurements. The problem is completely solved by maintaining the crystals in an atmosphere of saturated 1,4-Dioxane vapor. Thus, the sample mount used in neutron scattering experiments is sealed in an aluminium can with a small amount of deuterated solvent.

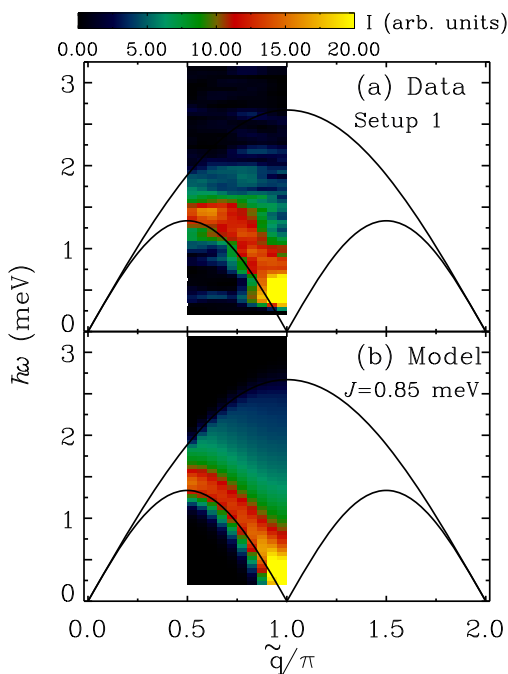


Figure 6. (a) False-color contour map of background subtracted inelastic neutron scattering intensity in $2\text{Dioxane} \cdot 2\text{D}_2\text{O} \cdot \text{CuCl}_2$ as a function of transferred energy $\hbar\omega$ and transferred wavevector along the chain \tilde{q} at $T=1.6$ K [49]. (b) Instrument resolution convolved model calculation of two-spinon continuum Müller approximation with $J=0.85$ meV. Solid lines are the predicted lower and upper bounds of the spinon continuum with $J=0.85$ meV.

An initial inelastic neutron scattering characterization of $2\text{Dioxane} \cdot 2\text{H}_2\text{O} \cdot \text{CuCl}_2$ was performed at the triple axes spectrometers TASP at PSI and SPINS at the NIST Center for Neutron Research (NCNR) [49]. Fig. 6(a) shows a false-color contour map of the measured spin excitation spectrum. These data confirm the simple AF spin chain nature of the material. In fact, the measured intensity can be attributed to a multi-particle continuum of so-called spinon excitations, which are a peculiarity of gapless one-dimensional quantum magnets [50]. A global fit to the data with the so-called Müller approximation [51] of this continuum, convolved with instrumental resolution, is shown in Fig. 6(b). The measurements allow us to determine key energy parameter of this system, namely the intra-chain exchange constant $J=0.85$ meV [49].

As an organic $S = 1/2$ AF chain compound with experimentally accessible energy scales, $2\text{Dioxane} \cdot 2\text{H}_2\text{O} \cdot \text{CuCl}_2$ is certainly not unique. Among several other representatives, Cu benzoate [52] and copper pyrazine dinitrate (CuPzN) [11] are perhaps the ones most extensively studied. What makes the new material special is that, unlike the needle-shaped CuPzN , it is very easy to grow into extremely large and compact single crystals. At the same time, unlike Cu-benzoate, it has the same g -tensor for all Cu^{2+} ions, which is critical for high-field experiments. This makes $2\text{Dioxane} \cdot 2\text{H}_2\text{O} \cdot \text{CuCl}_2$ a perfect material for investigating some very interesting yet subtle features of the excitation spectrum in applied magnetic fields. In particular, one expects the dynamic structure factor to obey universal finite-temperature scaling laws of the Tomonaga-Luttinger liquid model [53]. The scaling exponents are predicted to vary continuously with field [50]. An experimental verification of these predictions is technically challenging due to the expectedly

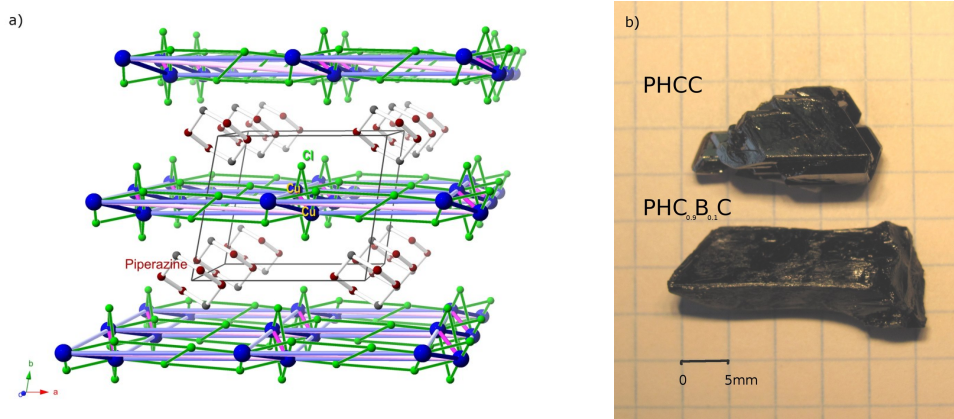


Figure 7. (a) Crystal structure of PHCC. Antiferromagnetic superexchange interactions are shown in purple (frustrated) and in blue (non-frustrated), with bond's strength increasing approximately with line weight. (b) Large single crystals of pure and 10% Br substituted PHCC grown by temperature gradient method.

very weak neutron scattering intensities. It will only be possible thanks to the very large deuterated samples available. These studies are currently underway.

2.3. A quasi-2D spin liquid

A significant number of quantum magnets fall into the category of *spin liquids* with a gapped spin excitation spectrum. In these materials, the only energy scale relevant for low energy physics is the gap Δ . Excitations from the non-magnetic spin liquid ground state across the gap can typically be described as dispersive spin-1 carrying quasiparticles - *magnons*. In the semiclassical picture, magnons are long-lived. At elevated temperatures their lifetimes are shortened by mutual collisions. Here dimensionality plays a crucial role. For one-dimensional systems, reduction of lifetime is the most prominent. Indeed, in $d = 1$, mutual collisions cannot be avoided regardless of the inter-magnon interaction strength. In the two-dimensional case, the details of the two-magnon potential become relevant. Magnon decay can also result from a spatially random *external* potential. Such a potential can be created, for example, by introducing random magnetic bonds. How will such disorder affect magnon dynamics?

To tackle this problem experimentally, we chose the quasi-two-dimensional quantum magnet piperazinium hexachlorodicuprate (PHCC). This material crystallizes in the triclinic space group $P\bar{1}$, with a rather large unit cell ($a = 6.0836(4)\text{\AA}$, $b = 7.0348(5)\text{\AA}$, $c = 7.9691(5)\text{\AA}$, $\alpha = 81.287(4)^\circ$, $\beta = 80.053(3)^\circ$, $\gamma = 68.917(3)^\circ$). It features $S = 1/2$ Cu^{2+} ions in a complex semi-frustrated network of exchange interactions. The latter are carried by Cu-Cl-Cl-Cu bonds in the crystallographic (ac)-planes (Fig.7a). The piperazinium molecules create an effective magnetic insulation layer between these planes. No inter-plane coupling has been detected to date. The magnetic properties of pure PHCC have been extensively studied. The value of the spin gap $\Delta=1$ meV, as well as all peculiarities of the spin excitation spectrum, are well established [15, 16, 54, 55]. Armed with this knowledge, we set out to introduce disorder in PHCC by substituting a fraction of the nonmagnetic exchange interaction-mediating Cl^- ions for the larger ionic radii Br^- . Such a substitution affects the relevant bond angles, and therefore to *locally* modulates the strength of superexchange interactions.

The growth of PHCC was first described in Ref. [56] and further characterized in Refs. [15, 57, 58]. To prepare large single crystals for neutron scattering exper-

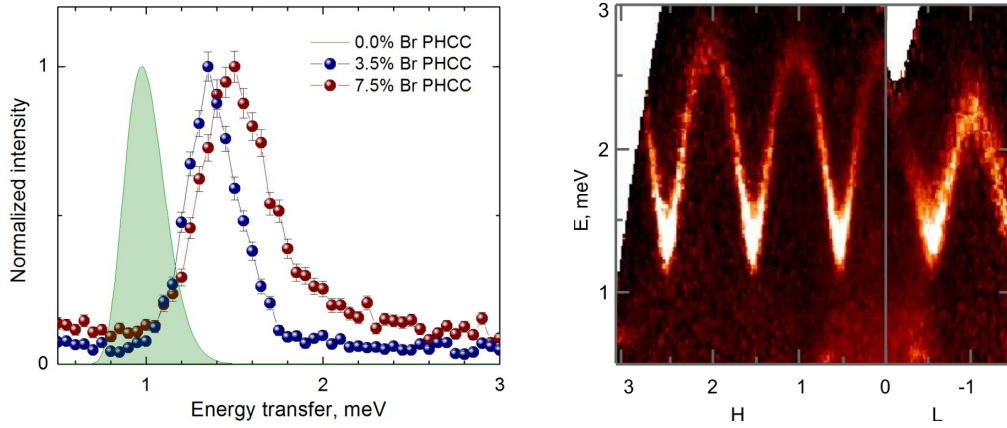


Figure 8. *Left:* Effect of disorder on magnon excitations at the antiferromagnetic zone centre $(0.5, 0.5, -0.5)$, measured at temperature 1.6 K. The green curve represents instrumental resolution and is a simulation for disorder-free PHCC based on the results of [54]. *Right:* The spin excitation spectrum measured on CNCS in a 3.5% Br PHCC sample, at 1.5 K.

iments we adopted the following procedure. i) Piperazine ($C_4D_{10}N_2$) and $CuCl_2$ powders are separately dissolved in concentrated deuteriochloric acid in a molar ratio 1:4 ii) PHCC powder is formed upon slowly adding the piperazine solution to the $CuCl_2$ one. iii) Seed crystals are grown using the temperature gradient method on a hotplate. The solution is kept at 15 degrees above room temperature. Small crystals appear on the cylinder walls. iv) The selected seed is suspended in the growth cylinder. Its surface as well as the cylinder walls are periodically cleared of spurious crystals. Using this method, in four weeks time, we have successfully grown single crystals of mass up to 2.8g (Fig.7b). Step-like features tend to form on crystal surfaces but the step's edges and faces remain strictly parallel to crystal's faces. Growth of disordered samples (PHCBC) follows exactly the same recipe with replacement of pure hydrochloric acid with mixture of HCl and HBr in desired ratio. Our focus is predominantly on small amount of disorder. Batches of crystals with 0.5%, 1%, 2.5%, 3.5%, 5%, 7.5%, 10% and 12.5% nominal Br concentration were synthesized. Powder and single crystal X-ray measurements confirmed all samples to be single phase crystals with lattice parameters that increase monotonically with Br content. Br concentrations beyond 13% in solution seem to lead to phase separation or other instabilities that inhibit crystal formation. For neutron scattering studies we replaced the hydrogen rich piperazine with fully deuterated isotopomer piperazine-d10. The acids were replaced with the respective deuterated heavy water solutions as well.

The effects of disorder on the magnon excitations are evident from inelastic neutron scattering experiment. Initial measurements were performed with triple axis spectrometer TASP (Fig.8). Compared to what was reported for the disorder-free material [54], the gap energy is increased. In addition, with increasing disorder, there is a clear broadening of the magnon line, well beyond the effect of experimental resolution. Our current efforts are focused on mapping the disorder effects across the Brillouin zone. In this task, the time-of-flight instrument CNCS at Oak Ridge National Laboratory has proven to be a most valuable tool, providing simultaneous access to large range of momentum transfers. Future plans include the study of the field induced quantum critical point in disordered PHCC.

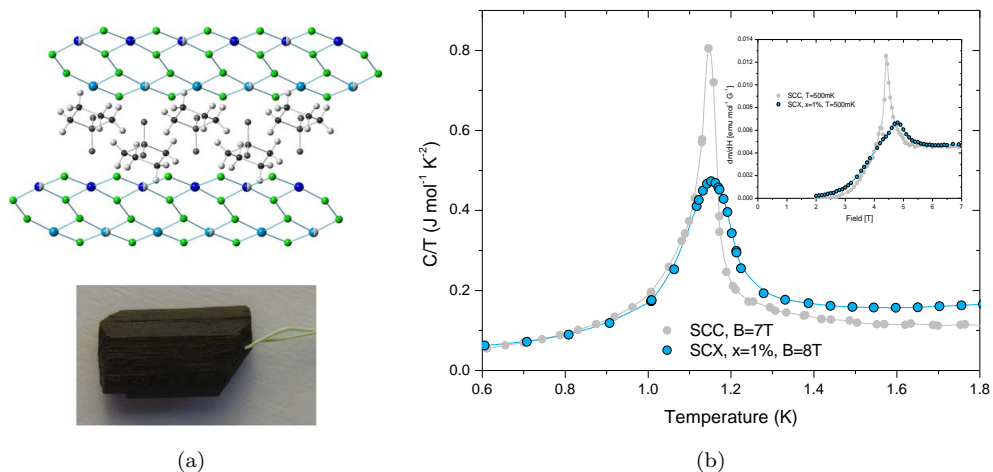


Figure 9. (a) Top: Four-leg spin ladders in $\text{H}_8\text{C}_4\text{SO}_2 \cdot \text{Cu}_2(\text{Cl}_{1-x}\text{Br}_x)_4$. The Cu^{2+} -ions (blue) interact (light blue lines) via the Cl^- or Br^- ions (green). The organic ligand is shown in gray. Bottom: An $x = 0.25\%$ $\text{H}_8\text{C}_4\text{SO}_2 \cdot \text{Cu}_2(\text{Cl}_{1-x}\text{Br}_x)_4$ crystal grown by the temperature gradient method. (b) Specific heat as a function of temperature (main panel) and magnetic susceptibility as a function of field (inset) measured in $\text{H}_8\text{C}_4\text{SO}_2 \cdot \text{Cu}_2(\text{Cl}_{1-x}\text{Br}_x)_4$ for $x = 0$ and $x = 0.012$ [61].

2.4. Frustration

A broad spectrum of exotic properties is expected to emerge in quantum spin systems with a *geometric frustration* of magnetic interaction. One such compound is $\text{H}_8\text{C}_4\text{SO}_2 \cdot \text{Cu}_2\text{Cl}_4$ (SCC for short). It crystallizes in a triclinic structure (space group No. 2, $\text{P}\bar{1}$) with the lattice constants $a = 9.39 \text{ \AA}$, $b = 10.76 \text{ \AA}$, $c = 6.62 \text{ \AA}$, $\alpha = 99.0^\circ$, $\beta = 95.2^\circ$ and $\gamma = 120.7^\circ$. The spin $S = 1/2$ -carrying Cu^{2+} ions are arranged in “4-leg spin ladders” that run along the crystallographic c axis (Fig. 9a). Magnetic interactions are through Cu-Cl-Cl-Cu superexchange pathways. As usual, the organic ligand acts as a filler ensuring excellent magnetic one-dimensionality of the Cu^{2+} subsystem. The network of antiferromagnetic interactions is rather complex and has a high degree of geometric frustration. As a result, for a long time, the physics of this material was misinterpreted [59, 60].

It was inelastic neutron experiments that revealed the true nature of the magnetic ground state and excitation spectrum. For this purpose, deuterated single crystals were grown at ORNL by slow evaporation as described in [59, 60, 62]. Copper (II) chloride was dissolved in deuterated ethanol and deuterated sulfolane ($\text{D}_8\text{C}_4\text{SO}_2$) was added to the solution. The solution was then slowly evaporated at 60°C until brown crystals were formed on the bottom of the growth beaker. We were never able to fully optimize this process, and the success rate remained below 50%. The resulting crystals were often somewhat irregular in shape, tending to form as elongated platelets with a maximal mass of about 200mg. In the end, a sufficient number of these could be assembled in a “supersample” of about 2 g total mass (Fig. 10B). Inelastic neutron data collected at the Disc Chopper Spectrometer at NIST NCNR (Fig. 10A) revealed a small energy gap of $\Delta \sim 0.5 \text{ meV}$ positioned at an *incommensurate* wave vector $\mathbf{q}\mathbf{c} = 0.48\pi$ (Fig. 10B) [63]. It was later shown that the system is best described in terms of a pair of coupled frustrated 2-leg ladders [64], and that incommensurability is a direct consequence of frustration. Furthermore, elastic neutron scattering experiments revealed that in an applied magnetic field $H_c = 3.75 \text{ T}$, the material goes through a quantum phase transition that is a Bose-Einstein condensation of magnons [18]. The high-field phase is an *incommensurate* quantum helimagnet.

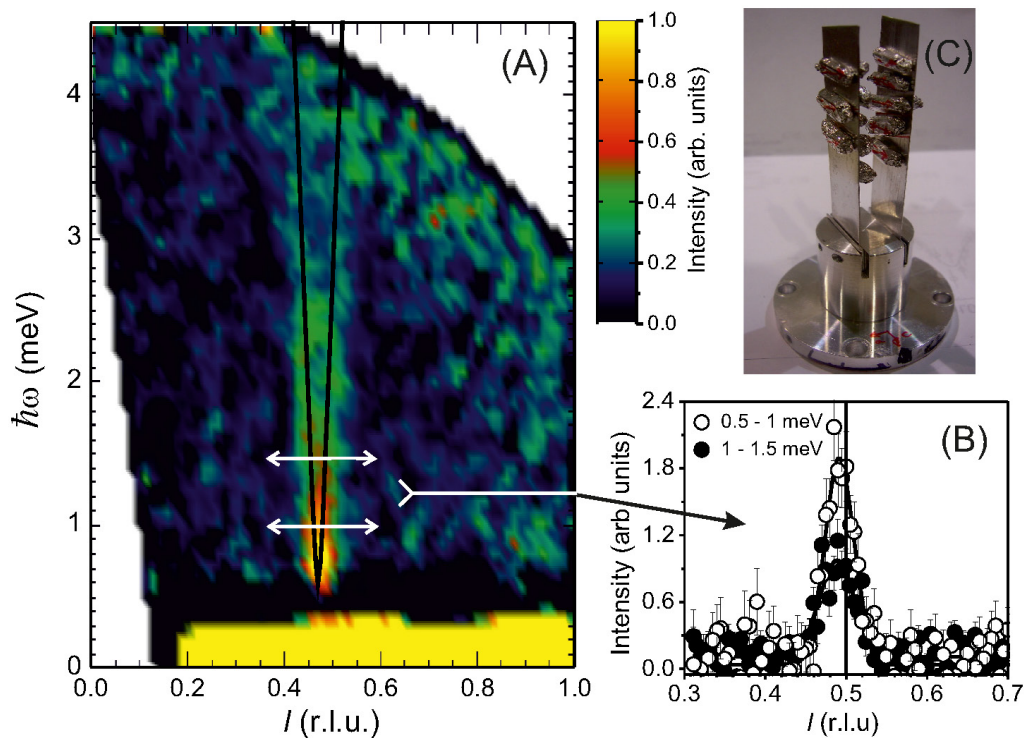


Figure 10. (A) Spin excitation spectrum of $D_8C_4SO_2 \cdot Cu_2Cl_4$ measured at 70mK using the DCS chopper spectrometer [63]. (B) Constant-energy cuts along the chain axis reveal the slightly incommensurate position of the magnon dispersion minimum. (C) Single crystal assembly consisting of 13 deuterated SCC crystals, used for this INS study.

A very interesting question is how this field-induced quantum phase transition is affected by bond randomness, of the type studied in PHCC (see above). We addressed this issue by a fabrication and systematic study of disordered Br-substituted crystals with the formula $H_8C_4SO_2 \cdot Cu_2(Cl_{1-x}Br_x)_4$, or SCX for short. In doing so, we switched to the temperature gradient growth method. For hot plate temperatures in the range $45^\circ C$ and 160° this approach yields much more reproducible results than slow evaporation. Compact and perfectly faceted crystals (Fig. 9a) with masses reaching 1 g were obtained at the ETHZ laboratory. The method works for Br concentrations x of up to about 12%. X-ray diffraction reveals a uniform distribution of substitution sites.

Given considerable investment made in deuterated reagents, it was quite *frustrating* to find that in the disordered material with Br concentrations as low as 1%, persistent neutron diffraction experiments failed to detect any sign of magnetic long range order in applied fields. Neither incommensurate nor commensurate Bragg reflections could be observed. This mystery was resolved in systematic low-temperature bulk measurements, for which the high quality of the temperature gradient grown samples was crucial. It turns out that even at very low Br content, field-induced 3-dimensional long-range ordering is indeed suppressed. In place of a sharp lambda-anomalies in specific heat curves and divergent magnetic susceptibility seen in the disorder-free compound, in the Br-substituted material one finds only broad features (Fig. 9B). We attribute this behavior to a novel disorder mechanism caused by *random geometric frustration* of magnetic interactions [61].

3. Summary

We would like to re-iterate our main message. In many cases, with patience and luck, even a quantum physicist can grow large crystals for neutron scattering studies, and then apply his or her true expertise to obtain high-quality data and new insight. Drawing the analogy between crystal growth and the culinary art, one can rephrase this as a quote from the famous 2007 animation feature “Ratatouille”: “Anybody can cook!”

4. Acknowledgements

The authors learned the techniques of sample growth described in this paper from their colleagues and collaborators, including M. B. Stone and B. Sales (Oak Ridge National Laboratory), C. L. Broholm (Johns Hopkins University), F. Xiao and C. Landee (Clark University), K. Katsumata (previously at RIKEN), H. Manaka (Kagoshima University), M. Hagiwara (Osaka University), P. Rey (CEA Grenoble) and many others. All recent measurements on the TASP spectrometer were facilitated by S. Gvasaliya and M. Mansson of ETHZ. We thank Paul Canfield (Ames National Lab) for support and useful comments and Dr. V. Glazkov (Kapitza Institute, Russian Acad. Sci.) for his involvement at the early stages of this project. Dr. T. Hong would like to point out that he was not involved in the part of the present project related to the DIMPY compound. Single-crystal X-ray diffraction work by RC was sponsored by the Division of Chemical Sciences, Geosciences and Biosciences, Office of Basic Energy Sciences, US Department of Energy. The research at Oak Ridge National Laboratory’s Spallation Neutron Source was sponsored by the Scientific User Facilities Division, Office of Basic Energy Sciences, U. S. Department of Energy. One of the authors (AZ), owes his interest in crystals to his father Acad. Prof. I. S. Zheludev and to his sister Prof. S. I. Zheludeva, both of whom were prominent Russian crystallographers. This work is partially supported by the Swiss National Fund under project 2-77060-11 and through Project 6 of MANEP.

References

- [1] Bertram N. Brockhouse Nobel Lecture. Nobelprize.org, 20 Sep 2011, http://www.nobelprize.org/nobel_prizes/physics/laureates/1994/brockhouse-lecture.html.
- [2] H.A. Bethe, *Z. Phys.* 71 (1931) p.256.
- [3] F.D.M. Haldane, *Phys. Rev. Lett.* 50 (1983) p.1153.
- [4] T.M. Rice, S. Gopalan and M. Sigrist, *Europhys. Lett.* 23 (1993) p.445.
- [5] G.S. Uhrig and H.J. Schulz, *Phys. Rev. B* 54 (1996) p.R9624–R9627.
- [6] S.R. White and I. Affleck, *Phys. Rev. B* 54 (1996) p.9862–9869.
- [7] I.A. Zaliznyak, C. Broholm, M. Kibune, M. Nohara and H. Takagi, *Phys. Rev. Lett.* 83 (1999) p.5370–5373.
- [8] S. Notbohm, P. Ribeiro, B. Lake, D.A. Tennant, K.P. Schmidt, G.S. Uhrig, C. Hess, R. Klingeler, G. Behr, B. Büchner, M. Reehuis, R.I. Bewley, C.D. Frost, P. Manuel and R.S. Eccleston, *Phys. Rev. Lett.* 98 (2007) p.027403.
- [9] T. Giamarchi, C. Rugg and O. Tchernyshev, *Nature Physics* 4 (2008) p.198.
- [10] L.P. Regnault, I. Zaliznyak, J.P. Renard and C. Vettier, *Phys. Rev. B* 50 (1994) p.9174.
- [11] M.B. Stone, D.H. Reich, C. Broholm, K. Lefmann, C. Rischel, C.P. Landee and M.M. Turnbull, *Phys. Rev. Lett.* 91 (2003) p.037205.
- [12] M. Kenzelmann, Y. Chen, C. Broholm, D.H. Reich, and Y. Qiu, *Phys. Rev. Lett.* 93 (2004) p.017204.
- [13] T. Masuda, A. Zheludev, H. Manaka, L.P. Regnault, J.H. Chung and Y. Qiu, *Phys. Rev. Lett.* 96 (2006) p.047210.
- [14] C. Rugg, B. Normand, M. Matsumoto, A. Furrer, D. McMorro, K.W. Kramer, H.U. Gudel, S.N. Gvasaliya, H. Mutka and M. Boehm, *Phys. Rev. Lett.* 100 (2008) p.25701.
- [15] M.B. Stone, I. Zaliznyak, D.H. Reich and C. Broholm, *Phys. Rev. B* 64 (2001) p.144405.
- [16] M.B. Stone, C. Broholm, D.H. Reich, O. Tchernyshyov, P. Vorderwisch and N. Harrison, *Phys. Rev. Lett.* 96 (2006) p.257203.

- [17] T. Hong, S.N. Gvasaliya, S. Herringer, M.M. Turnbull, C.P. Landee, L.P. Regnault, M. Boehm and A. Zheludev, *Phys. Rev. B* 83 (2011) p.052401.
- [18] V.O. Garlea, A. Zheludev, K. Habicht, M. Meissner, B. Grenier, L.P. Regnault and E. Ressouche, *Physical Review B* 79 (2009) p.060404.
- [19] J. Renard, M. Verdaguer, L. Regnault, W. Erkelens, J. Rossat-Mignod, J. Ribas, W. Stirling and C. Vettier, *J. Appl. Phys.* 63 (1988) p.3538.
- [20] I.A. Zaliznyak, L.P. Regnault and D. Petitgrand, *Phys. Rev. B* 50 (1994) p.15824.
- [21] A. Zheludev, S.E. Nagler, S.M. Shapiro, L.K. Chou, D.R. Talham and M.W. Meisel, *Phys. Rev. B* 53 (1996) p.15004.
- [22] A. Zheludev, V.O. Garlea, L.P. Regnault, H. Manaka, A. Tsvetik and J.H. Chung, *Phys. Rev. Lett.* 100 (2008) p.157204.
- [23] A. Zheludev, Y.C. Z. Honda, C. Broholm and K. Katsumata, *Phys. Rev. Lett.* 88 (2002) p.077206.
- [24] M. Hagiwara, L.P. Regnault, A. Zheludev, A. Stunault, N. Metoki, T. Suzuki, S. Suga, K. Kakurai, Y. Koike, P. Vorderwisch, and J.H. Chung, *Phys. Rev. Lett.* 94 (2005) p.177202.
- [25] V.S. Zapf, D. Zocco, B.R. Hansen, M. Jaime, N. Harrison, C.D. Batista, M. Kenzelmann, C. Niedermayer, A. Lacerda and A. Paduan-Filho, *Phys. Rev. Lett.* 96 (2006) p.077204.
- [26] V.O. Garlea, A. Zheludev, T. Masuda, H. Manaka, L.P. Regnault, E. Ressouche, B. Grenier, J.H. Chung, Y. Qiu, K. Habicht, K. Kiefer and M. Boehm, *Phys. Rev. Lett.* 98 (2007) p.167202.
- [27] B. Thielemann, C. Rüegg, H.M. Rønnow, A.M. Läuchli, J.S. Caux, B. Normand, D. Biner, K.W. Krämer, H.U. Güdel, J. Stahn, K. Habicht, K. Kiefer, M. Boehm, D.F. McMorrow and J. Mesot, *Phys. Rev. Lett.* 102 (2009) p.107204.
- [28] S.H. Glarum, S. Geschwind, K.M. Lee, M.L. Kaplan and J. Michel, *Phys. Rev. Lett.* 67 (1991) p.1614–1617.
- [29] G.E. Granroth, S. Maegawa, M.W. Meisel, J. Krzystek, L.C. Brunel, N.S. Bell, J.H. Adair, B.H. Ward, G.E. Fanucci, L.K. Chou, and D.R. Talham, *Phys. Rev. B* 58 (1998) p.9312.
- [30] Y. Uchiyama, Y. Sasago, I. Tsukada, K. Uchinokura, A. Zheludev, T. Hayashi, N. Miura and P. Boni, *Phys. Rev. Lett.* 83 (1999) p.632.
- [31] L.C. Tippie and W.G. Clark, *Phys. Rev. B* 23 (1981) p.5846–5853.
- [32] H. Manaka, I. Yamada, M. Hagiwara and M. Tokunaga, *Phys. Rev. B* 63 (2001) p.144428.
- [33] H. Manaka, A.V. Kolomietz and T. Goto, *Phys. Rev. Lett.* 101 (2008) p.077204.
- [34] T. Hong, Y.H. Kim, C. Hotta, Y. Takano, G. Tremelling, M.M. Turnbull, C.P. Landee, H.J. Kang, N.B. Christensen, K. Lefmann, K.P. Schmidt, G.S. Uhrig and C. Broholm, *Phys. Rev. Lett.* 105 (2010) p.137207.
- [35] G.L. Squires *Introduction To The theory Of Thermal neutron Scattering*, Cambridge University Press, 1978.
- [36] V.F. Sears, *Neutron News* 3 (1992) p.26–37.
- [37] G. Dhanaraj, K. Byrappa, V. Prasad and M. Dudley (eds.) *Handbook of Crystal Growth*, Springer-Verlag, 2010.
- [38] B.R. Patyal, B.L. Scott and R.D. Willett, *Phys. Rev. B* 41 (1990) p.1657.
- [39] E. Dagotto, *Rep. Prog. Phys.* 62 (1999) p.1525.
- [40] C. Rüegg, K. Kiefer, B. Thielemann, D.F. McMorrow, V. Zapf, B. Normand, M.B. Zvonarev, P. Bouillot, C. Kollath, T. Giamarchi, S. Capponi, D. Poilblanc, D. Biner and K.W. Krämer, *Phys. Rev. Lett.* 101 (2008) p.247202.
- [41] B. Thielemann, C. Rüegg, K. Kiefer, H.M. Rønnow, B. Normand, P. Bouillot, C. Kollath, E. Orignac, R. Citro, T. Giamarchi, A.M. Läuchli, D. Biner, K.W. Krämer, F. Wolff-Fabris, V.S. Zapf, M. Jaime, J. Stahn, N.B. Christensen, B. Grenier, D.F. McMorrow and J. Mesot, *Phys. Rev. B* 79 (2009) p.020408.
- [42] A. Shapiro, C.P. Landee, M. Turnbull, J. Jornet, M. Deumal, J. Novoa, M. Robb and W. Lewis, *J. Am. Chem Soc* 129 (2007) p.952–959.
- [43] J.J. Somoza, M. Deumal, M.M. Turnbull and J.J. Novoa, *Polyhedron* 28 (2009) p.1965.
- [44] D. Schmidiger, S. Mühlbauer, S.N. Gvasaliya, T. Yankova and A. Zheludev, *Phys. Rev. B*, in press arXiv:1105.4832v1 (2011).
- [45] D. Schmidiger, S. Mühlbauer, P. Bouillot, S. Gvasaliya, G. Ehlers, A. Zheludev, T. Giamarchi and C. Kollath *et al.*, In preparation .
- [46] G. Ehlers, A.A. Podlesnyak, J.L. Niedziela, E.B. Iverson and P.E. Sokol, *Rev. Sci. Instr.* 82 (2011) p.085108.
- [47] Y. Ajiro, T. Asano, T. Inami, H. Aruga-Katori and T. Goto, *J. Phys. Soc. Jpn.* 63 (1994) p.859.
- [48] J.C. Livermore, R.D. Willett, R.M. Gaura and C.P. Landee, *INorg. Chem.* 21 (1982) p.1403.
- [49] T. Hong, R. Custelcean, B.C. Sales, B. Roessli, D.K. Singh and A. Zheludev, *Phys. Rev. B* 80 (2009) p.132404.
- [50] T. Giamarchi *Quantum Physics in One Dimension*, Clarendon Press, 2003.
- [51] G. Muller, H. Thomas, M.W. Puga and H. Beck, *J. Phys. C* 14 (1981) p.3399.
- [52] D.C. Dender, *Spin Dynamics in the Quasi-One-Dimensional $S=1/2$ Heisenberg Antiferromagnet Copper Benzoate*, Johns Hopkins University, 1997.
- [53] A. Tsvetik *Quantum Field Theory in Condensed Matter Physics*, Cambridge University Press, 2007.
- [54] M.B. Stone, C. Broholm, D.H. Reich, P. Schiffer, O. Tchernyshyov, P. Vorderwisch and N. Harrison, *New Journal of Physics* 9 (2007) p.31.
- [55] M.B. Stone, I.A. Zaliznyak, T. Hong, C.L. Broholm and D.H. Reich, *Nature* 440 (2006) p.187–190.
- [56] G. Marcotrigiano, L. Menabue and G.C. Pellacani, *Inorganic Chemistry* 15 (1976) p.2333–2336.
- [57] A. Daoud, A.B. Salah, C. Chappert, J.P. Renard, A. Cheikhrouhou, T. Duc and M. Verdaguer, *Phys. Rev. B* 33 (1986) p.6253–6260.
- [58] L.P. Battaglia, A.B. Corradi, U. Geiser, R.D. Willett, A. Motori, F. Sandrolini, L. Antolini, T. Manfredini, L. Menabue and G.C. Pellacani, *J. Chem. Soc., Dalton Trans.* (1988) p.265–271.
- [59] M. Fujisawa, J.I. Yamaura, H. Tanaka, H. Kageyama, Y. Narumi and K. Kindo, *Journal of the Physical Society of Japan* 72 (2003) p.694–697.
- [60] M. Fujisawa, H. Tanaka and T. Sakakibara, *Progress of Theoretical Physics Supplement* 159 (2005)

- p.212–216.
- [61] E. Wulf, S. Mühlbauer, T. Yankova and A. Zheludev, Disorder instability of the magnon condensate in a frustrated spin ladder; arXiv:1110.0806v1 [cond-mat.str-el].
 - [62] D. Swank and R. Willett, *Inorganica Chimica Acta* 8 (1974) p.143–148.
 - [63] V.O. Garlea, A. Zheludev, L.P. Regnault, J.H. Chung, Y. Qiu, M. Boehm, K. Habicht and M. Meissner, *Physical Review Letters* 100 (2008) p.037206.
 - [64] A. Zheludev, V.O. Garlea, A. Tsvelik, L.P. Regnault, K. Habicht, K. Kiefer and B. Roessli, *Phys. Rev. B* 80 (2009) p.214413.